EFFECT OF PRECOATING ON PROPERTIES OF FUNCTIONAL COATING AND ELECTRICAL CONDUCTIVITY OF INKJET-PRINTED ELECTRONICS

JURAJ GIGAC, MÁRIA FIŠEROVÁ and ALBERT RUSS

Pulp and Paper Research Institute, Dúbravská cesta 14, 841 04 Bratislava, Slovak Republic
✉ *Corresponding author: J. Gigac, gigac@vupc.sk*

Received October 27, 2022

In the present work, various surface treatments of base paper were investigated in order to make it suitable for application in printed electronics. A functional coating based on silica pigment was preceded by PVOH-containing precoating, and differently surface treated papers were characterized in terms of surface roughness, relative area of surface pores, wettability, printability and by FTIR spectroscopy. The precoating had a significant effect on the constriction of through-pores, the reduction of their number, and on the permeability of the functional coating, and it increased the dynamic contact angle of the liquids. Analysis of FTIR spectra of precoated and functionally coated paper confirmed a higher content of polyvinyl alcohol binder and cationic polymer in the functional coating, compared to that of functionally coated paper, without precoating. SEM analysis showed that the silver layer of the RFID antenna printed by inkjet on the precoated and functionally coated paper was continuous. Better printability of the precoated and functionally coated paper, compared to the functionally coated paper, without precoating, was also confirmed by higher electrical conductivity of the dipole of the RFID antenna, which reached the level of the antenna printed on a commercial inkjet PET film.

Keywords: coated paper, inkjet printing, RFID antenna, electrical conductivity, FTIR, SEM

INTRODUCTION

Printed RFID antennas are usually applied to different plastic films[1-3] or paper substrates.[4-12] Paper is the most available and the cheapest substrate material, which has been widely used in various paper-based electronics.[13-15] Other significant advantages of paper include recyclability, light weight, biodegradability, environmental friendliness and low coefficient of thermal expansion.[16] Easy biodegradability does not mean poor mechanical toughness, durability and stability of paper substrates.[17] Hence, reasonable physicochemical strategies should be applied to optimize the surface characterization and mechanical flexibility, such as coating with kaolin, chromatogenic grafting, and extruding a polymer film.[18-19]

Printability is an important property of paper products and can be a differentiating factor in terms of their production and printing technology. Ordinary papers are porous and have a rougher surface than the plastic film used to print electronics. To modify the surface of the paper, it is possible to use the processes of coating and smoothing in a calender[20-21] or a hot stamping machine. Smoothing in a hot stamping machine achieved a higher bending stiffness of coated paperboards compared to calendering.[22] The paper surface is usually coated with a dispersion coating consisting of mineral pigments and organic binders. The smoothness of the paper surface depends on the composition of coatings, the amount and layers of the coating and the final surface finish. Depending on the composition of coatings, properties such as surface roughness, porosity, permeability and wettability can be varied.[20,23-24] The surface properties of papers can be adjusted at the same time to achieve the desired functional properties, such as water, oil and grease resistance, low vapour and gas permeability,[25-29] and flame retardation.[30] Low-temperature plasma processing of surfaces and interfaces is an interesting option for applications in flexible and printed electronics where surface

cleaning, activation or functionalization are required.[31-32]

Aluminum RFID antennas produced by the chemical etching technique have a thickness of 9-16 μm. Thermal transfer printing with Metallograph® conductive ribbon is a simple, fast and economical method of digital printing for electronic circuits, sensors and RFID antennas.[33] Compared to printing techniques, such as screen printing, flexography, gravure and inkjet printing, which use pastes and inks containing mostly silver nanoparticles (AgNPs), thermal transfer printing uses aluminum, which is about two orders of magnitude less costly for the equivalent conductivity of silver. Additionally, there are no fluids, no printing set-up, no drying and no sintering of the AgNPs. Without these additional steps, the process has a very small footprint and takes less than a second to accomplish. Thermal transfer printing of electronic devices in industrial thermal transfer printers is a new technology compared to inkjet technology. Companies SPF-Inc., IIMAK, Flexcon, QuickLabel, Graphic Marking Systems, Zebra, Insulectro, Steinerfilm, UPM Raflatac, Rain RFID, Voyantic participate in its development and applications.

Inkjet printing is still used as it is a rapidly developing technique, able to compete with conventional printing techniques and is widely used for the production of printed electronics. Inkjet printing is a digital and contactless technique that contains almost no chemical waste, and allows the use of paper or plastic substrates. It is ideal for fast prototyping and promises high throughput and low cost. Inks composed of metal nanoparticles are widely used in the area of inkjet-printed flexible sensors for conductive or sensitive layers. Due to their high surface-to-volume ratio, their post-sintering temperature is much lower than that of the corresponding bulk materials. For example, the sintering temperature of silver nanoparticle ink is 150–250 °C, which is much less than that of bulk silver materials (>700 °C). Optimum inkjet printing quality was achieved if the paper surface was able to rapidly absorb the solvent (water) from the ink and the AgNPs remained anchored on the surface. This was achieved in coating compositions with pigments based on alumina, precipitated calcium carbonate and silica. The presence of large pores enabled rapid absorption of the ink solvent. Large surface area of the pigment with fine pores combined with the cationic polymer PDADMAC enabled the fixation of AgNPs on the surface. The application of the cationic polymer PDADMAC in the functional hydrophilic coating of paper substrates had a positive effect on the electrical resistance of silver antennas printed by inkjet technology. Electrical conductivity of inkjet-printed UHF RFID antennas increased after calendering the coated papers, however, as the basis weight of the coating on the paper increased, the electrical conductivity of the antennas decreased.[20] While in thermal transfer printing, the addition of cationic polymers to coating compositions did not play any role, their addition as well as their type was decisive in inkjet printing. UHF RFID antennas printed on smooth functional coated paper with a functional hydrophilic coating based on inorganic pigments did not reach the electrical conductivity achieved on PET film for inkjet printing.[21]

The barrier precoat increased the dimensional stability of the paper, enabled the efficient placement of AgNPs of ink on the surface of the functional hydrophilic coating and thereby increasing the electrical conductivity of the silver antenna to the level that is achieved on PET films for inkjet printing. The composition of the functional hydrophilic coating and its calendering had a positive effect on the surface smoothness, electrical conductivity and quality of UHF RFID antennas printed by thermal transfer and inkjet printing. Uncalendered papers and calendered papers with higher surface roughness (optical surface variability above 6%) provided only non-conductive antennas.[21] Inkjet printing methods are of rising interest to extended scientific areas, taking benefit of advances made in related fields (technological innovations, nanochemistry, supramolecular chemistry, *etc*.) and feeding dynamic fields of applications, such as optoelectronics, energy harvesting and biomedical devices.[34]

The aim of this work was the characterization of experimentally coated papers in terms of surface roughness, relative area of surface pores, wettability, printability with inkjet ink containing AgNPs and by FTIR spectroscopy.

EXPERIMENTAL

Materials

Base paper (denoted as sample a) used for coating experiments was commercial wood-free coated paper for offset printing (basis weight 100 $g.m^{-2}$). Functionally coated papers were denoted as (b1) and (b2), while precoated and functionally coated papers – as (c1) and (c2).

The precoat contained PVOH (polyvinyl alcohol) Mowiol 6-88 (partially hydrolyzed).

Coating colours of functional coating contained silica pigment Sipernat 310 (ground precipitated SiO_2) and PVOH (Mowiol 6-88) in a ratio of 60/40 (b1, c1) or 40/60 (b2, c2). The addition of 2.5 wt% of cationic polymer PDADMAC and 0.2 wt% of surfactant Dynol 810 per pigment to the coating colours was the same. PDADMAC (polydiallyldimethylammonium chloride) with the Mw 200,000–350,000 $g.mol^{-1}$ was purchased from Sigma Aldrich and surfactant Dynol 810 (ethoxylated 2,5,8,11-tetramethyl-6-dodecyn-5,8 diol) – from Evonic Operations GmbH.

A Novele PET (polyethylene terephthalate) film, from NovaCentrix, was used as a reference substrate. Inkjet ink Metalon JS-B25P containing AgNPs was also received from NovaCentrix.

UHF RFID antenna design for inkjet printing: DogBone, the dimensions of the antenna were 94 x 24 mm (Smartrac division of the company Avery Dennison).

Methods

Coating

The precoat and functional coatings were prepared by applying the coating colours to base papers using a #4 metering rod and drying at 120 °C in an oven. The basis weight of the precoat was 1.8-2.1 $g.m^{-2}$ and of the functional coatings was 2.8-3.1 $g.m^{-2}$.

Calendering

Calendering of papers with functional coatings (b1, b2, c1, c2) was performed using an FUS 80 laboratory calender (Kleinewefers GmbH, Germany) by two passes between paper and metal cylinder, at a linear load in the nip of 260 $kN.m^{-1}$, a temperature of 80 °C and a speed of 5 $m.min^{-1}$. The coated side was in contact with the heated metal cylinder.

Inkjet printing, sintering and electrical conductivity of UHF RFID antenna

UHF RFID antenna printing was performed with an Epson Stylus C88+ piezoelectric inkjet printer. Sintering (curing) of inkjet-printed antenna was carried out at downforce of 75 kPa of the metal plate heated to 130 °C for 15 seconds. The printability and functionality of the antenna were evaluated using SEM microscopy of the printed surface and electrical conductivity. The electrical conductivity of the antenna dipole was calculated from the electrical resistance measured with a UNIT-T multimeter, Model UT70B.

Photoclinometry

Surface roughness OVS_{CLINO} (Optical Variability of Surface) of papers was evaluated by the photoclinometric method.[35] Photoclinometry describes the process of transformation of a 2D surface image into a map of various height levels. Incident light creates shadows (different gray levels). Paper is an anisotropic material; therefore, it is necessary to obtain surface images from at least two directions: machine direction (MD) and cross direction (CD). An average value was calculated from these values. The paper surface was scanned using a charge-coupled device (CCD) Nikon Coolpix E4500 camera (Nikon Corporation, Japan) by inclined illumination at 10° from MD and CD. Optical variability of the surface was calculated from image analysis using the ImageJ program.

SEM microscopy

The method of scanning electron microscopy at high magnification was used to evaluate the relative surface pore area of the functional coating and the uniformity of the sintered silver layer in an inkjet-printed antenna. Samples were prepared for SEM microscopy, by gold sputtering their surface using a Balzers SCD 040 sputtering device, in 0.15 bar vacuum for a period of 40 seconds with 50 mA electric current. For obtaining SEM images, a JEOL 760F scanning electron microscope, equipped with a Schottky thermo emission cathode (thermal FEG–W platting by ZrO_2) and with energy and wavelength dispersive spectrometers (Oxford Instruments), was used. The images were achieved with the following specifications: magnification X10,000, accelerating voltage 2 kV, work distance 7.9 mm, image size 2530 x 1890 pixels, image resolution 0.005 $\mu m.pixel^{-1}$.

The distribution of light and dark image areas obtained by SEM microscopy and by the photoclinometric method was evaluated using ImageJ software. Optical variability of surface, OVS_{SEM}, is expressed as the coefficient of variation of the original SEM image histogram, and it contains summarized information about the relative area of surface pores. The coefficient of variation expresses the ratio of surface pores area to the total surface area.[36]

Contact angle of liquids

Paper wettability can be determined by the contact angle of a liquid drop on its surface. Initial and dynamic contact angle (ICA and DCA) of liquids on papers were measured using an OCA 35 optical tensiometer (DataPhysics Instrument, Germany) by the sessile drop method. The contact angle was recorded by a CCD camera at the sequence of 20 $frames.s^{-1}$, from the first contact of the liquid drop with the paper surface (50 ms) through 5 seconds. Surface tension of test liquids: water – 72.8 $mN.m^{-1}$, 16% and 30% aqueous solutions of isopropyl alcohol (IPA) – 44.2 $mN.m^{-1}$ and 34.0 $mN.m^{-1}$, respectively. Contact angle was calculated as the average of 10 parallel measurements.

FTIR spectroscopy

Infrared spectra of papers were recorded in the middle region by the attenuated total reflection (ATR) technique, using a Nicolet iS 10 spectrometer.

Measurement conditions: ZnSe crystal, 128 scans, resolutions 2 cm^{-1}.[36]

RESULTS AND DISCUSSION

Characterization of papers

In the present study, functionally coated, and precoated and functionally coated papers, with calendered functional coatings, for inkjet printing of UHF RFID antennas were prepared and analyzed. The surface roughness, relative area of surface pores, wettability and ATR-FTIR spectra of the calendered coated papers were analysed. In addition, the printability of the thus-modified papers was evaluated using SEM microscopy and their functionality was assessed in terms of electrical conductivity of UHF RFID antennas.

Surface roughness and relative area of surface pores

The surface properties of the base paper (a), functionally coated papers with calendered functional coatings (b1, b2), and precoated and functionally coated papers with calendered functional coatings (c1, c2) are shown in Table 1. The base paper has the surface roughness, OVS_{CLINO}, of 7.3% and the relative area of surface pores, OVS_{SEM}, of 19.4%, which corresponds to the high quality of wood-free coated paper with the printing roughness of Parker Print Surf (PPS) of 0.94 μm. PPS roughness was calculated from the equation: $PPS = 0.103\ OVS_{CLINO} + 0.192$.[21] Functionally coated papers (b1, b2) had the surface roughness of 5.5% and 4.7%, and the relative area of surface pores of 27.1 and 26.2%, respectively. Precoated and functionally coated papers (c1, c2) had the surface roughness of 5.1% and 4.7%, and a relative area of surface pores of 26.8 and 27.6%, respectively. ImageJ analysis of SEM images of the surface of the functional coating of functionally coated papers, and of those precoated and functionally coated did not confirm the expected large changes in the relative area of the surface pores.

Wettability

The print quality is mostly affected by the equilibrium wetting, which can be determined by the liquid contact angle. The surface tension of the liquid, the surface energy of the paper and the environmental conditions determine the contact angle. The wettability of papers was determined by the contact angle of a liquid drop on their surface. The values of initial contact angles (ICA) and dynamic contact angles (DCA) of water, as well as 16% and 30% aqueous solutions of isopropyl alcohol, on papers are shown in Table 2. The ICA was measured at 50 ms and the DCA at 5 s from the first contact of the liquid with the surface of the paper. The base paper (a) had a hydrophobic surface (ICA of water 101°), while the papers with a calendered functional coating had a hydrophilic surface (ICA of water 72-78°). It follows from the above that the type of base paper for coating had no effect on the ICA of the liquids on the functional coatings. The DCA of water of the precoated and functionally coated papers (c1, c2) was twice as high (66-67°) as that of the functionally coated papers without precoating (b1, b2). We assume that the smaller decrease in the DCA of water in the case of precoated and functionally coated papers was caused by the constriction of the through-pores, by reducing their number and the permeability of the functional coating. The analysis of DCA of liquids showed that the geometry and number of through-pores in the functional coating were significantly influenced by the base paper type.

Table 1
Surface roughness and relative area of surface pores for base paper, functionally coated paper, as well as precoated and functionally coated paper

Properties / Papers	Surface roughness OVS_{CLINO} (%)	Relative area of surface pores OVS_{SEM} (%)
Base paper (a)	7.3	19.4
Functionally coated paper		
(b1)	5.5	27.1
(b2)	4.7	26.2
Precoated and functionally coated paper		
(c1)	5.1	26.8
(c2)	4.7	27.6

Table 2
Contact angles of liquids on base paper, functionally coated, and precoated and functionally coated papers

Papers / Contact angles	Base paper	Functionally coated paper		Precoated and functionally coated paper	
	(a)	(b1)	(b2)	(c1)	(c2)
ICA of water in 50 ms (°)	101	72	78	75	76
DCA of water in 5 s (°)	82	33	37	66	67
ICA of 16% IPA in 50 ms (°)	51	38	42	40	42
DCA of 16% IPA in 5 s (°)	28	24	27	38	40
ICA of 30% IPA in 50 ms (°)	30	22	27	29	31
DCA of 30% IPA in 5 s (°)	8	11	11	27	30

Similar differences in DCA between functionally coated papers (b1, b2), and those precoated and functionally coated (c1, c2) were also found when using 16% and 30% aqueous solutions of isopropyl alcohol with lower surface tension (44.2 and 34 $mN.m^{-1}$). The surface tension of inkjet inks containing metal nanoparticles ranges from 28 to 53 $mN.m^{-1}$.[37-38]

ATR-FTIR spectra

Figure 1 illustrates the ATR-FTIR spectra of base paper (a), functionally coated papers with a calendered SiO_2/PVOH functional coating in a ratio of 60/40 (b1) or of 40/60 (b2), as well as those of precoated and functionally coated papers with a PVOH precoat and with a calendered SiO_2/PVOH functional coating in a ratio of 60/40 (c1) or of 40/60 (c2). The addition of the cationic polymer PDADMAC to the coating colour of the functional coatings was the same.

Figure 1 (a) shows the ATR-FTIR spectrum of commercial coated wood-free paper, which was used as a base paper in the preparation of papers for printed electronics. In the absorption spectrum of the base paper (a), bands with maxima at wavenumbers 3694, 3654 and 3620 cm^{-1} are observed. According to the literature,[39] the absorption bands at 3697, 3669, 3645 cm^{-1} and 3620 cm^{-1} are typical of the kaolinite spectrum (amount of aluminum in the octahedral). The band around 3620 cm^{-1} has been ascribed to internal hydroxyls, and the peaks at the other three characteristic wavenumbers are generally attributed to vibration of external hydroxyls. The high peak at 1386 cm^{-1} corresponds to the aromatic C=C stretching vibration and clearly explains the chemical structures of the cellulose in the base paper, which matches with the band at 1387 cm^{-1} in the FTIR spectra of mixtures of nanocrystalline cellulose with PVOH.[40] Absorption bands were also detected at 1032, 1008 cm^{-1} and 914 cm^{-1}, typical of the vibration of O-H group (Al-O-H) and Si-O bond (Si-O-Si) in kaolin. Also, the bands at 871 cm^{-1} and 712 cm^{-1} were detected. These are characteristic of the vibration of C=O group in CO_3^{2-} ions of calcium carbonate, which, together with kaolin, form the inorganic part in coated graphic papers.[36]

Figure 1 (b1, b2) presents the ATR-FTIR spectra of functionally coated papers, which were prepared by coating the base paper (a) with a mixture of SiO_2/PVOH in the ratio of 60/40 (b1) or of 40/60 (b2), with addition of PDADMAC. In both spectra, the intensity of the peak at 1386 cm^{-1} decreased significantly, absorption bands appeared at 3343 cm^{-1} and 1086-1089 cm^{-1}, typical of the vibration of the O-H group in PVOH and of the Si-O bond in SiO_2, respectively; the band at 1730 cm^{-1} corresponding to the vibration of the C=O group in PVOH and the band at 939 cm^{-1}, which represents the stretching vibration of the C-H methyl group in PDADMAC, were also noted. In addition, in the spectrum of functionally coated paper (b2) with a higher proportion of PVOH, the band corresponding to C-O stretching vibration in PVOH appeared at 1236 cm^{-1}.

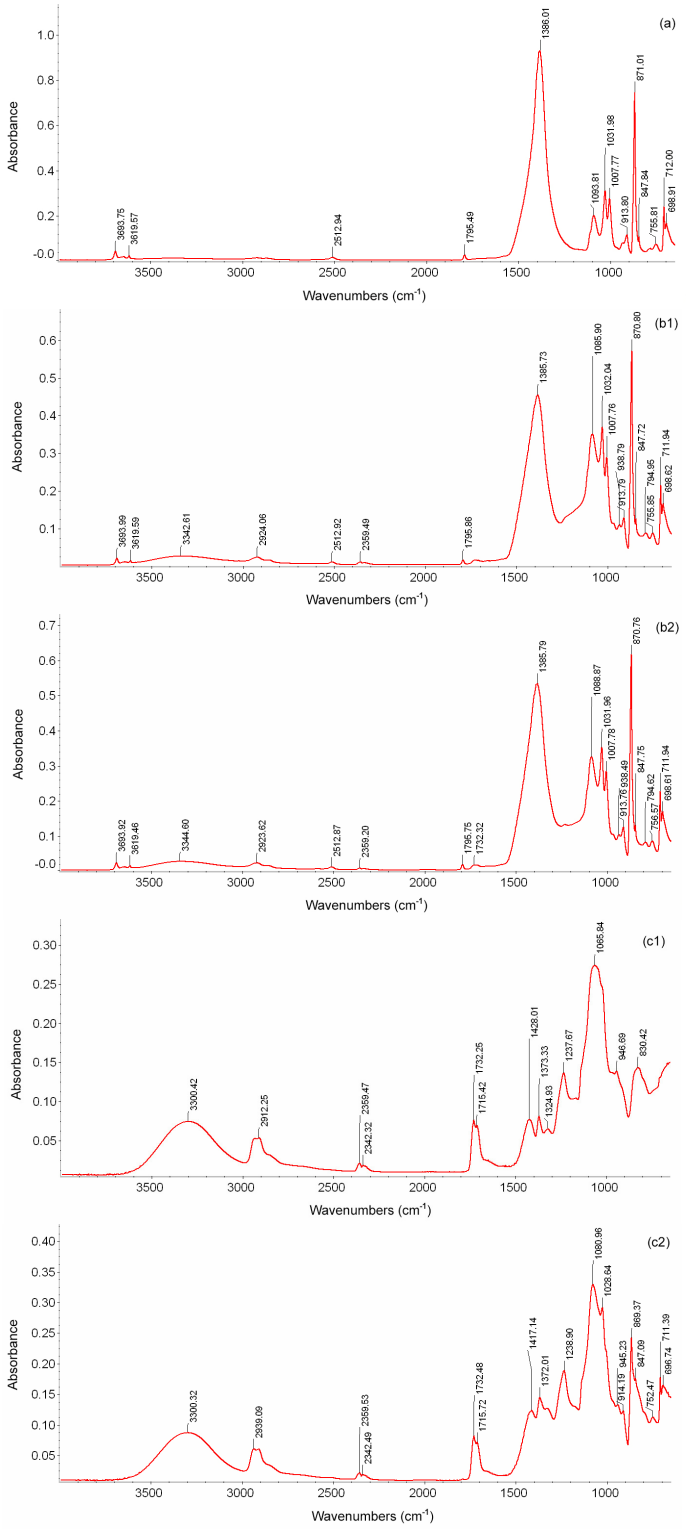

Figure 1: ATR-FTIR spectra of base paper (a), functionally coated papers (b1, b2), and precoated and functionally coated papers (c1, c2)

ATR-FTIR spectra of precoated and functionally coated papers with calendered functional coatings are shown in Figure 1 (c1, c2). The precoated and functionally coated papers were prepared by coating a base paper with a PVOH precoat and a functional coating from a mixture of SiO_2/PVOH in the ratio of 60/40 (c1) or 40/60 (c2), with the addition of PDADMAC. In both absorption spectra, there is a broad band at 3300 cm^{-1}, corresponding to the vibration of the O-H group, a band in the region of 2938-2939 cm^{-1}, corresponding to the vibration of the methylene group CH_2 in PDADMAC, bands at wavenumbers 2912 cm^{-1} and 1715 cm^{-1}, corresponding to the vibration of the carbonyl group C=O in PVOH, and a band at 1238-1239 cm^{-1}, corresponding to C-O stretching vibrations in PVOH. Absorption bands were also observed at wavenumbers 1066 and 1081 cm^{-1} and in the region 830-847 cm^{-1}, corresponding to Si-O-Si vibrations, and a band at 945-947 cm^{-1} typical of vibrations of the CH_2 methylene group in PDADMAC. In precoated and functionally coated papers c1 and c2, the bands corresponding to the vibration of the methylene group CH_2 in PDADMAC appeared at 1428 cm^{-1} and 1417 cm^{-1}, which could be related to a higher concentration of PDADMAC in the functional coatings of these papers in comparison with those of functionally coated papers b1 and b2, which do not present these bands. The stretching vibration of the C-N bond in PDADMAC was localised at 1174 cm^{-1} in the absorption spectrum of precoated and functionally coated paper c1, and to a lesser extent in the precoated and functionally coated paper c2. Cationic polymer PDADMAC showed bands at wavenumbers 2945, 1477 cm^{-1} and 961 cm^{-1}, caused by the stretching and bending vibrations of methylene CH_2 and methyl C-H groups.[41-42] In the spectrum of the quaternary amine PDADMAC, a band was observed at 1137 cm^{-1}, which corresponds to the stretching vibration of the C-N bond.[43]

In Table 3, the results of the ATR-FTIR spectral analysis of the base paper (a), functionally coated papers (b1, b2) and precoated and functionally coated papers (c1, c2) are compared with the results of other research works focusing on the surface treatment of paper with mixtures of silica (SiO_2) or nanocrystalline cellulose (NCC), with a binder based on PVOH or cationic polymer PDADMAC,[40-47] as well as with other results in the field of coated and uncoated paper.[36,39]

Printability of paper and electrical conductivity of printed antennas

Precoated and functionally coated papers (c1, c2), with a PVOH precoat and calendered functional coating based on silica pigment, were more suitable for inkjet printing of conductive structures than functionally coated papers (b1, b2), without PVOH precoat. Better printability of precoated and functionally coated paper (c1) was confirmed by the SEM image of the printed surface of a UHF RFID antenna (Fig. 2), as well as by the higher electrical conductivity of inkjet-printed UHF RFID antennas (Fig. 3).

In Figure 2, the SEM images of the sintered silver layer of the UHF RFID antennas printed by the inkjet technique on functionally coated (b1), and on precoated and functionally coated (c1) papers, as well as on a Novele PET film. The sintered AgNPs on the functionally coated paper (b1) formed a discontinuous layer, while on the precoated and functionally coated paper (c1) and on the PET film, they formed a continuous conductive layer.

In Figure 3, the electrical conductivities of the silver UHF RFID antennas printed on functionally coated paper (b1), precoated and functionally coated paper (c1), and Novele PET film are compared. The electrical conductivity of the dipole of the antenna, with a discontinuous layer of silver was 94 $mS.cm^{-1}$. The continuous conductive layer of silver formed on the precoated and functionally coated paper (c1) increased electrical conductivity to 480 $mS.cm^{-1}$, which is comparable to the electrical conductivity of 565 $mS.cm^{-1}$ achieved on the Novele PET film.

From the comparison of ATR-FTIR spectra (Fig. 1) obtained for the functionally coated papers (b1, b2), and precoated and functionally coated papers (c1, c2), it can be noted that in the spectra of precoated and functionally coated papers, the bands corresponding to the vibration of the methylene group CH_2 in PDADMAC were present at wavenumbers 1428 cm^{-1} and 1417 cm^{-1}. These bands are not found in the ATR-FTIR spectra of the functionally coated papers, without precoating, even though PDADMAC was present in the coating colour for the functional coating in the same amount as in the case of the precoated and functionally coated papers.

Table 3
ATR-FTIR spectra of base paper (a), functionally coated papers (b1, b2), as well as precoated and functionally coated papers (c1, c2)

Functional group	Wavenumber, cm^{-1}	Material	References
CH2 stretching of methylene group	2900; 2907	PVOH; PVOH+SiO_2	44; 48; 40
C-H stretching and bending of methyl group	939 (b1, b2), 947, 2939 (c1, c2); 2945, 1477, 961; 960; 967	PDADMAC	41; 42; 49
	1428 (c1), 1417 (c2); 1421, 1475; 1479		47; 42
C-N stretching	1174 (c1, c2)	PDADMAC	
	1137	PDADMAC	43
	1165; 1159; 1105;	polymers with quaternary amine	46; 42; 41
C=C stretching of aromatic group	High peak 1386 (a), half peak 1386 (b1, b2)	cellulose	
	1387	NCC+PVOH	40
O-H stretching in (Al-O-H)	3694, 3654, 3620 (a, b1, b2)	kaolin	39
	1032, 1008, 914 (a)	kaolin	36
Si-O stretching in (Si-O-Si)	1066 (c1), 1081 (c2); 1066	PVOH+SiO_2	48
	830-847 (c1, c2); 798	PVOH+SiO_2	44
C=O stretching in CO_3^{2-} ion	871, 712 (a)	$CaCO_3$	36
O-H stretching	3343(b1, b2); 3300 (c1, c2); 1086-9 (b1, b2)	PVOH+SiO_2	48; 40
C=O stretching	2912 (c1, c2); 2917	PVOH+SiO_2; PVOH	48
	1730 (b1, b2) 1715 (c1, c2); 1720	PVOH+SiO_2 polymers with quaternary amine	46
C-O stretching	1236 (b2), 1238-1239 (c1, c2)	PVOH	
	1230	PVAc	45

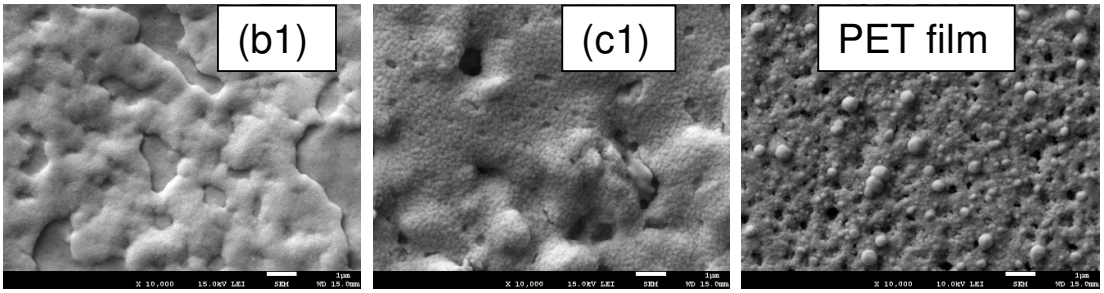

Figure 2: SEM images of the sintered silver layer of UHF RFID antennas inkjet-printed on functionally coated paper b1 (left), precoated and functionally coated paper c1 (center), and Novele PET film (right)

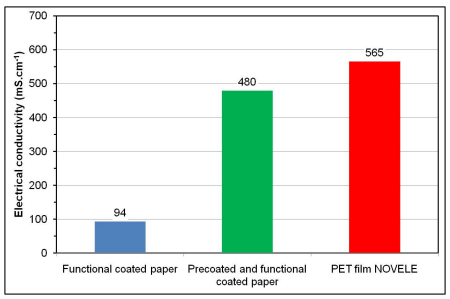

Figure 3: Comparison of electrical conductivity of silver UHF RFID antennas inkjet-printed on functionally coated paper, precoated and functionally coated paper and Novele PET film

Based on the above, we assume that the precoat created a physical barrier against the leakage of the binder PVOH and the cationic polymer PDADMAC from the coating colour of the functional coating into the base paper, and thereby ensured the effective fixation of AgNPs from the inkjet ink on the surface of the precoated and functionally coated paper. This also explains the increase in the electrical conductivity of the dipole of silver antennas.

The inferior quality of functionally coated paper with the functional coating (b1) to that of precoated and functionally coated paper (c1) was confirmed by SEM images (Fig. 2), as well as by the conductivities of the inkjet-printed UHF RFID antennas (Fig. 3). We assume that the worse printability and lower electrical conductivity of the UHF RFID antennas were caused by the lower concentration of the PVOH binder and the cationic polymer PDADMAC on the surface of the functional coating (b1). The lower content of PDADMAC in the functional coating does not allow sufficient fixation of the AgNPs from the inkjet ink on the surface of functionally coated paper.

Similar results were achieved when printing UHF RFID antennas using the inkjet technique on papers with a PVOH precoat and functional coatings based on precipitated calcium carbonate.[21]

CONCLUSION

The analysis of the FTIR spectra revealed that the type of surface treatment applied to base paper (precoating and functional coating or just functional coating) is an important factor influencing the quality of coated papers. The analysis of the FTIR spectra allowed the identification of the components of the functional coating and explained the causes of the differences in the electrical conductivity of the printed antennas.

Paper that was surface treated by precoating followed by functional coating met the conditions required for printing UHF RFID antennas, had better printability, as confirmed by SEM images of the silver layer, and the printed antenna had higher electrical conductivity compared to that printed on functionally coated paper, without precoating.

The results of the FTIR analysis showed that functionally coated paper contained less binder PVOH and cationic polymer PDADMAC in the functional coating than precoated and functionally coated paper. Thus, it could be concluded that the precoat created a physical barrier against the leakage of PVOH and PDADMAC from the functional coating to the base paper.

The precoat on the base paper provided a simple and inexpensive way to prepare inkjet paper, presenting suitable printability for UHF RFID antennas, at the level of the commercial inkjet PET film. This fact can be explained by the analogy between precoated and functionally coated paper and a non-porous PET film with a functional layer. The advantage of the precoated and functionally coated paper is its lower environmental footprint, compared to that of the PET film.

Spectroscopic methods, especially IR, can be thus used to optimize the composition and properties of base paper and functional coating, with an emphasis on the effective use of natural materials and inkjet ink with metal nanoparticles.

ACKNOWLEDGMENT: This work was supported by the Slovak Research and Development Agency under contract No. APVV-19-0029.

REFERENCES

[1] K. C. Chin, C. H. Tsai, L. C. Chang, C. L. Wei, W. T. Chen *et al.*, in *Procs. Printed Circuits Expo. Apex and the Designers Summit*, 2008, pp. 1940-1946

[2] K. Janeczek, in *Procs. XII International PhD Workshop OVD*, Poland, 2010, pp. 345-348

[3] A. Arazna, K. Janeczek and K. Futera, *Circuit World*, **43**, 9 (2017), https://doi.org/10.1108/CW-10-2016-0047

[4] S. Merilampi, L. Ukkonen, L. Sydanheimo, P. Ruuskanen and M. Kivikoski, *Int. J. Antennas Propag.*, **2007**, ID 090762 (2007), https://doi.org/10.1155/2007/90762

[5] A. Rida, Y. Li, R. Vyas and M. M. Tentzeris, *IEEE Antennas Propag. Mag.*, **51**, 13 (2009)

[6] V. Lakafosis, A. Rida, R. Vyas, Y. Li, S. Nikolaou *et al.*, in *Procs. IEEE*, October 2010, **98**, 1601 (2010), https://doi.org/10.1109/JPROC.2010.2049622

[7] J. Xi, H. Zhu and T. T. Ye, in *Procs. 2011 IEEE International Conference on RFID*, pp. 38-44, https://doi.org/10.1109/RFID.2011.5764634

[8] R. Zichner and R. R. Baumann, in *Procs. LOPE-C 2011*, Messe Frankfurt, Germany, pp. 361-363

[9] T. Öhlund and M. Andersson, in *Procs. LOPE-C 2012*, January 2012, pp. 115-119

[10] R. Bollström and M. Toivakka, in *Procs. 15th Fundamental Research Symposium*, Cambridge, UK, September 2013, pp. 945-966

[11] U. Kavčič, M. Pivar, M. Dokič, D. G. Svetec, L. Pavlovič *et al*., *Mater. Technol*., **48**, 261 (2014)
[12] H. He, L. Sydänheimo, J. Virkki and L. Ukkonen, *Int. J. Antennas Propag*., **2016**, ID 9265159 (2016), https://doi.org/10.1155/2016/9265159
[13] F. C. Loghin, A. Falco, A. Albrecht, J. F. Salmeron, M. Becherer *et al*., *ACS Appl. Mater. Interfaces*, **10**, 34683 (2018), https://doi.org/10.1021/acsami.8b08050
[14] P. Zhu, Y. Liu, Z. Fang, Y. Kuang, Y. Zhang *et al*., *Langmuir*, **35**, 4834 (2019), https://doi.org/10.1021/acs.langmuir.8b04259
[15] S. Li, N. Pan, Z. Zhu, R. Li, B. Li *et al*., *Adv. Funct. Mater*., **29**, 1807343 (2019), https://doi.org/10.1002/adfm.201807343
[16] R. Alrammouz, J. Podlecki, P. Abboud, B. Sorli and R. Habchi, *Sens. Actuat. A Phys*., **2018**, 209 (2018), https://doi.org/10.1016/j.sna.2018.10.036
[17] X. Wang, M. Zhang, L. Zhang, J. Xu, X. Xiao *et al*., *Mater. Today Commun*., **31**, 103263 (2022), https://doi.org/10.1016/j.mtcomm.2022.1032636
[18] S. Wünscher, R. Abbel, J. Perelaer and U. S. Schubert, *J. Mater. Chem. C*, **2**, 10232 (2014), https://doi.org/10.1039/C4TC01820F
[19] M. Schmid, S. Sängerlaub, O. Miesbauer, V. Jost, J. Werthan *et al*., *Polymers*, **2014**, 2764 (2014), https://doi.org/10.3390/polym6112764
[20] J. Gigac, M. Fišerová, M. Kováč and M. Stankovská, *Wood Res*., **65**, 25 (2020), https://doi.org/10.37763/wr.1336-4561/65.1.025036
[21] J. Gigac, M. Fišerová and S. Hegyi, *Wood Res*., **66**, 71 (2021), https://doi.org/10.37763/wr.1336-4561/66.1.7184
[22] J. Gigac and M. Fišerová, *Wood Res*., **67**, 26 (2022), https://doi.org/10.37763/wr.1336-4561/67.1.2640
[23] J. Gigac, M. Stankovská, M. Letko and E. Opálená, *Wood Res*., **59**, 717 (2014)
[24] J. Gigac, M. Stankovská, M. Fišerová and E. Opálená, *Wood Res*., **60**, 739 (2015)
[25] Z. Long, M. Wu, H. Peng, L. Dai, D. Zhang *et al*., *BioResources*, **10**, 7907 (2015), https://doi.org/10.15376/biores.10.4.7907-7920.
[26] U. V. Brodnjak and D. Todorova, *J. Polym. Text. Eng*., **4**, 33 (2017)
[27] R. A. Ilyas, S. M. Sapuan, M. R. Ishak, E. S. Zainudin, M. S. N. Atikah *et al*., in *Procs. 6th Postgraduate Seminar on Natural Fiber Reinforced Polymer Composites*, Malaysia, December, 2018, pp. 55-59
[28] S. Kopacic, A. Walzl, A. Zankel, E. Leitner and W. Bauer, *Coatings*, **8**, 235 (2018), https://doi.org/10.3390/coatings 8070235
[29] J. Gigac, M. Stankovská and M. Fišerová, *Wood Res*., **63**, 871 (2018)
[30] R. Sonnier, A. Taguet, L. Ferry and J.-M. Cuesta, "Towards Bio-Based Flame Retardant Polymers", Briefs in Molecular Science, Springer, 1st ed., 2018, pp. 47-58
[31] J. Vida and T. Homola in *Procs. 2nd International Conference and Advanced Surface Enhancement* (*INCASE 2021*), Singapore, September 7-8, 2021, pp. 63-67
[32] J. Gigac, M. Fišerová and R. Tiňo, *Wood Res*., **67**, 671 (2022), https://doi.org/10.37763/wr.1336-4561/67.4.671685
[33] J. Gigac, M. Fišerová, M. Kováč and S. Hegyi, *Mater. Technol*., **55**, 277 (2021)
[34] J. Lemarchand, N. Bridonneau, N. Battaglini, F. Carn, G. Mattana *et al*., *Angew. Chem. Int. Ed*., **61**, 1 (2022), https://doi.org/10.1002/anie.202200166
[35] M. Kasajová and J. Gigac, *Nord. Pulp Pap. Res. J*., **28**, 443 (2013), https://doi.org/10.3183/NPPRJ-2013-28-03-p443-449
[36] J. Gigac, M. Kasajová, M. Maholányiová, M. Stankovská and M. Letko, *Nord. Pulp Pap. Res. J*., **28**, 274 (2013), https://doi.org/10.3183/NPPRJ-2013-28-02-p274-281
[37] C. M. Dang, K. K. Huynh and D. M. T. Dang, *Biol. Chem. Res*., **6**, 126 (2019)
[38] L. Mo, Z. Guo, L. Yang, Q. Zhang, Y. Fang *et al*., *Int. J. Mol. Sci*., **20**, 2124 (2019), https://doi.org/10.3390/ijms20092124
[39] V. Hospodarova, E. Singovszka and N. Stevulova, *Am. J. Anal. Chem*., **9**, 303 (2018), https://doi.org/10.4236/ajac.201896023
[40] S. Yenidoğan, *Mater. Sci*., **26**, 317 (2020), https://doi.org/10.5755/j01.ms.26.3.21499
[41] S. Jareansin, P. Sukaam and B. Kusuthanm, *Polym. Bull*., **76** 4507 (2019), https://doi.org/10.1007/s00289-018-2603-8
[42] A. Hebeish and S. Sharaf, *RSC Adv*., **5**, 103036 (2015), https://doi.org/10.1039/C5RA07076G
[43] L. Padhye, Y. Luzinova, M. Cho, B. Mizaikoff, J.-H. Kim *et al*., *Environ. Sci. Technol*., **45**, 4353 (2015), https://dx.doi.org/10.1021/es104255e
[44] M. F. H. Al-Kadhemy, S. A. Ibrahim and J. A. S. Salman, *AIP Conf. Procs*., **2290**, 050013 (2020), https://doi.org/10.1063/5.0028817
[45] R. P. D´Amelia, L. Huang and J. Mancuso, *World J. Chem. Ed*., **7**, 1 (2019), https://doi.org/10.12691/wjce-7-1-1
[46] X. Lv, Ch. Liu, S. Song, Y. Quiao, Y. Hu *et al*., *RSC Adv*., **8**, 2941 (2018), https://doi.org/10.1039/c7ra11001d
[47] L. Wang, Y. Chen and Z. Zhang, in *Procs. 17th IAPRI World Conference on Packaging*, 2010, pp. 418-421
[48] T. Pirzada, S. A. Arvidson, C. D. Saquinng, S. S. Shah and S. A. Khan, *Langmuir*, **28**, 5834 (2012), https://doi.org/10.1021/la300049j
[49] I. Yudovin-Faber, N. Beyth, E. I. Weiss and A. J. Domb, *J. Nanopart. Res*., **12**, 591 (2010), https://doi.org/10.1007/s11051-009-9628-8